According to the Flory–Huggins theory, the higher the degree of polymerization of the polyol and the lower the value of the H_1–polyol interaction parameter, the higher the polyol concentration as well as T_{ME} of the eutectic composition. In contrast to the PEO and PTMO systems, poly(propylene oxide) (PPO) is intrinsically an amorphous compound and forms a crystalline–amorphous phase diagram with H_1.

Wide angle X-ray diffraction revealed that the presence of the polyol, as well as variations in temperature up to the liquidus point, did not alter the crystal form of H_1. This suggests that the melting point depression observed is a result of the excess free energy released during mixing, which allows determination of the H_1/polyol interaction parameter using Scott's equation. The interaction parameter densities of H_1/polyol pairs at their melting points were found to be $B_{H_1/PEO} = -4.63$ cal/cm^3, $B_{H_1/PTMO} = -3.41$ cal/cm^3, and $B_{H_1/PPO} = -1.21$ cal/cm^3. The negative values of B indicate H_1 and the polyols (PEO, PTMO, and PPO) form compatible liquids.

The morphology of H_1/polyol blends was studied with a polarizing microscope. Distinct spherulites were observed for pure H_1 and H_1/polyol blends. With the addition of polyols, the spherulite radii increase and the texture of the spherulites change from maltese cross patterns to radiating fibrous morphologies, especially for those blends that are of high PEO or PTMO content. The spherulites of H_1/PEO systems are larger in size than those of H_1/PTMO or H_1/PPO. This may be due to the fact that H_1 and PEO possess a strong interaction (suggested by the low value of $B_{H_1/PEO}$) which makes PEO a more effective diluent for hindering nucleation in H_1. In addition, the presence of PEO may also ease the transport of the crystallizing H_1 units across the liquid–crystal interface, resulting in larger spherulites.

Acknowledgment. We acknowledge partial support of this work by the Polymers Section of the NSF Division of Materials Research through Grant DMR 81-06888 and by the Naval Air Systems Command through Contract N00019-82-C-0246. We also thank Jen Kai Chen for carrying out part of the thermal analysis study.

Registry No. H_1, 10097-16-2; PEO, 25322-68-3; PPO, 25322-69-4; PTMO, 25190-06-1.

References and Notes

(1) S. L. Cooper and G. M. Estes, Eds., "Multiphase Polymers", American Chemical Society, Washington, DC, 1979, Adv. Chem. Ser. No. 176.
(2) R. Bonart and E. H. Muller, *J. Macromol. Sci. Phys.*, **B10**, 345 (1974).
(3) J. W. C. Van Bogart, Ph.D. Dissertation, University of Wisconsin, 1981.
(4) Y. Camberlin, and J. P. Pascault, *J. Polym. Sci., Polym. Chem. Ed.*, **21**, 415 (1983).
(5) Y. Camberlin, J. P. Pascault, M. Letoffe, and P. Caludy, *J. Polym. Sci., Polym. Chem. Ed.*, **20**, 383 (1982).
(6) J. Blackwell and K. H. Gardner, *Polymer*, **20**, 13 (1979).
(7) J. Blackwell, M. R. Nagarajan, and T. B. Hoitink, *Polymer*, **23**, 950 (1982).
(8) J. Blackwell and M. Ross, *J. Polym. Sci., Polym. Lett. Ed.*, **17**, 447 (1979).
(9) H. Tadokoro, Y. Chatani, T. Yoshihara, S. Tohara, and S. Murahashi, *Makromol. Chem.*, **73**, 109 (1964).
(10) C. P. Buckley and A. J. Kovacs, *Colloid Polym. Sci.*, **254**, 695 (1976).
(11) H. Tadokoro, Y. Takahashi, Y. Chatani, and H. Kakida, *Makromol. Chem.*, **109**, 96 (1967).
(12) H. Kakida, D. Makino, Y. Chatani, M. Kobayashi, and H. Tadokoro, *Macromolecules*, **3**, 569 (1970).
(13) R. L. Scott, *J. Chem. Phys.*, **17**, 279 (1949).
(14) T. Nishi and T. T. Wang, *Macromolecules*, **8**, 909 (1975).
(15) R. L. Imken, D. R. Paul, and J. W. Barlow, *Polym. Eng. Sci.*, **16**, 593 (1976).
(16) T. Nishi, *J. Macromol. Sci., Phys.*, **B17**, 517 (1980).
(17) W. W. Wendlandt, "Thermal Methods of Analysis", Wiley, New York, 1974.
(18) K. Nakayama, T. Ino, and I. Matsubara, *J. Macromol. Sci., Chem.*, **A3**, 1005 (1969).
(19) J. C. Wittmann and R. St. John Manley, *J. Polym. Sci., Polym. Phys. Ed.*, **15**, 2277 (1977).
(20) C. B. Wang and S. L. Cooper, *Macromolecules*, **16**, 775 (1983).
(21) L. Mandelkern, "Crystallization of Polymers", McGraw-Hill, New York, 1964.
(22) K. K. S. Hwang, G. Wu, S. B. Lin, and S. L. Cooper, *J. Polym. Sci., Polym. Chem. Ed.*, accepted for publication.
(23) T. T. Wang and T. Nishi, *Macromolecules*, **10**, 42 (1977).
(24) J. I. Lauritzen, Jr. and J. D. Hoffman, *J. Appl. Phys.*, **44**, 4340 (1973).

Miscibility of Ethylene–Vinyl Acetate Copolymers with Chlorinated Polyethylenes. 3. Simulation of the Spinodal Using the Equation of State Theory

Shamsedin Rostami and David J. Walsh*

Department of Chemical Engineering and Chemical Technology, Imperial College, London SW7, England. *Received June 20, 1983*

ABSTRACT: Chlorinated polyethylene and ethylene–vinyl acetate copolymers have previously been shown to be miscible and to phase separate on heating. In this paper a spinodal equation based on Flory's equation of state theory was derived and applied to the phase diagrams of these mixtures. Using values of the interactional parameter, X_{12}, derived from heats of mixing measurements, it was found that the predicted spinodal curves could not match the cloud point curves unless the entropy correction term containing Q_{12} was used. Also the predicted curves were flatter than the cloud points, suggesting an overestimation of X_{12}. The excess volume change on mixing was also calculated and was found to be larger than the measured value. This can also be improved by introducing Q_{12} and by using a lower value of X_{12}.

Introduction

In previous papers we have described the miscibility of various ethylene–vinyl acetate copolymers (EVA) with chlorinated polyethylenes (CPE).[1,2] This was demonstrated by the presence of single glass transition temperatures intermediate between those of the pure polymers. We also have measured the cloud point curves of the mixtures.[1] They phase separate on heating, showing a lower critical solution temperature (LCST). The LCST was higher for polymers with a higher content of vinyl

0024-9297/84/2217-0315$01.50/0

acetate units or with a higher degree of chlorination, respectively, showing that such polymers are "more miscible" when they contain a higher concentration of interacting groups.

The postulated specific interaction between these polymers involves the carbonyl group of the EVA and the methine proton of the CPE.[3] This was demonstrated from a shift in the carbonyl IR adsorption frequency. Furthermore the shift decreased at higher temperatures, suggesting that the specific interaction dissociates at higher temperatures.

The heats of mixing of low molecular weight analogues have been measured and were found to be favorable for mixing (negative).[2] They also were found to decrease at higher temperatures, which is consistent with the idea of dissociation of the specific interaction. Measurements using inverse gas chromatography also showed less favorable interaction parameters at higher temperatures.

Thermodynamic theories of polymer miscibility are in principle capable of predicting or describing phase separation behavior. The theoretical phase diagram consists of a binodal curve which is the line connecting the equilibrium compositions of phase-separated mixtures and is given by

$$(\Delta\mu_1)_A = (\Delta\mu_1)_B \qquad (\Delta\mu_2)_A = (\Delta\mu_2)_B \tag{1}$$

where $(\Delta\mu_i)_A$ and $(\Delta\mu_i)_B$ are the chemical potentials of component i in phases A and B, relative to its potential in the neat state, on the binodal at a given temperature. The spinodal curve lies inside the binodal, represents the limits of metastable compositions, and is given by

$$\partial^2(\Delta G)/\partial\Phi^2 = 0 \tag{2}$$

The spinodal and the binodal meet at the cricital point where

$$\partial^3(\Delta G)/\partial\Phi^3 = \partial^2(\Delta G)/\partial\Phi^2 = 0 \tag{3}$$

Polymer compositions between the binodal and the spinodal can separate by nucleation and growth, whereas within the spinodal fluctuations in concentration are stable and phase separation may occur spontaneously by spinodal decomposition. The observed cloud point curve therefore should lie between the binodal and the spinodal. If phase separation occurs at the spinodal, this fact may possibly be inferred from the morphology of the phase-separated structure.

Using a modified version of the equation of state theory developed by Flory and his collaborators,[4-6] McMaster[7] examined the contribution of the pure- and binary-state parameters to the miscibility of hypothetical polymer–polymer mixtures. He observed that the theory is capable of predicting both lower and upper critical solution temperature behavior individually or simultaneously. Olabisi[8] has applied McMaster's treatment to a real system of poly(caprolactone) and poly(vinyl chloride). Using a simpler form of McMaster's derivation, ten Brinke et al.[9] have studied the effect of binary parameters on the asymmetrical shape of the spinodal curves.

In this paper we have attempted to use the thermodynamic data described earlier[2] along with other derived and measured thermodynamic properties, and, using a modified version of the equation of state theory, to simulate the spinodal curves to match the cloud point curves obtained for EVA/CPE mixtures.[1]

The results can be compared with those obtained by one of us and other workers in simulating the phase diagrams of mixtures of various polyacrylates with chlorinated polyethylene.[10,11]

Theory

With the notation of Flory and his collaborators,[4-6] and as shown in the Appendix, the equation for the spinodal, based purely on the chemical potential of the mixture, can be derived. In this derivation the pressure effect on the phase boundary is considered, whereas the effect of polydispersity is neglected. The pure and binary state equation is given by

$$\tilde{P}\tilde{v}/\tilde{T} = \tilde{v}^{1/3}/(\tilde{v}^{1/3} - 1) - 1/\tilde{T}\tilde{v} \tag{4}$$

At atmospheric pressure this equation yields

$$\tilde{T} = (\tilde{v}^{1/3} - 1)/\tilde{v}^{4/3} \tag{5}$$

with $\tilde{v}$ being

$$\tilde{v}^{1/3} = (3 + 4\alpha T)/(3 + 3\alpha T) \tag{6}$$

These three equations are equally applicable to the mixture and pure components where α values are substituted accordingly, and

$$\tilde{T} = T/T^* = (\Phi_1 P^*_1 \tilde{T}_1 + \Phi_2 P^*_2 \tilde{T}_2)/P^* \tag{7}$$

$$P^*_i = \gamma_i T \tilde{v}_i^2 \qquad i = 1, 2 \tag{8}$$

$$P^* = \Phi_1 P^*_1 + \Phi_2 P^*_2 - \Phi_1\Theta_2 X_{12} \tag{9}$$

$$\Phi_2 = W_2 v^*_{2sp}/(W_2 v^*_{2sp} + W_1 v^*_{1sp}) \qquad \Phi_1 = 1 - \Phi_2 \tag{10}$$

$$\Theta_2 = (S_2/S_1)\Phi_2/((S_2/S_1)\Phi_2 + \Phi_1) \qquad \Theta_1 = 1 - \Theta_2 \tag{11}$$

In the equation of state theory of Flory and his collaborators the residual free energy of mixing of a mixture is given by

$$G^R_M = \Delta H_M - T\Delta S^R_M \tag{12}$$

where

$$\Delta H_M = \bar{r}NV^*[\Phi_1 P^*_1/\tilde{v} + \Phi_2 P^*_2/\tilde{v} - P^*/\tilde{v}] \tag{13}$$

$$-T\Delta S^R_M = 3rNV^*[\Phi_1 P^*_1 \tilde{T}_1 \ln(\tilde{v}_1^{1/3} - 1)/(\tilde{v}^{1/3} - 1) + \Phi_2 P^*_2 \tilde{T}_2 \ln(\tilde{v}_2^{1/3} - 1)/(\tilde{v}^{1/3} - 1)] \tag{14}$$

The residual chemical potential change on mixing is given by

$$\Delta\mu_1/RT = P^*_1 V^*_1/RT[3\tilde{T}_1 \ln(\tilde{v}_1^{1/3} - 1)/(\tilde{v}^{1/3} - 1) + 1/\tilde{v}_1 - 1/\tilde{v} + \tilde{P}_1(\tilde{v} - \tilde{v}_1)] + V^*_1 X_{12}\Theta_2^2/RT\tilde{v} \tag{15}$$

To conform the theoretical prediction of eq 12–15 with experimental results the entropy term $-\bar{r}NV^*Q_{12}\Theta_2\Phi_1$ must be added to eq 12 and similarly the term $-TQ_{12}V^*_1\Theta_2^2$ must be added to eq 15. Further details and full derivations of these equations are given in ref 12.

Materials

The physical properties, material characterization, code names, and other experimental data of the polymers, analogues, and blends referred to in this paper were described in papers 1 and 2 of this series.[1,2] The values used in this paper are summarized in Table I.

Parameters Used in the Simulation

Application of this theory to a binary mixture requires the following state parameters of pure components: (a) the specific volume, $v_{sp} = 1/d$; (b) the thermal expansion coefficient, $\alpha = (1/v)(\partial v/\partial T)_P$; (c) the thermal pressure coefficient, $\gamma = (\partial P/\partial T)_V$. And it requires the following binary parameters: (d) the surface per unit of core volume ratio, S_2/S_1; (e) the interaction term, X_{12}.

The specific volumes of pure components were obtained by equal density titration as described in ref 13. Mixtures of saturated sodium bromide solution and distilled water were used for the titration of CPE. Mixtures of 1-propanol and distilled water were used for the titration of EVA45.

Table I

compd	code name	Cl content, %	$\bar{M}_w$	$\bar{M}_n$	$\bar{M}_w/\bar{M}_n$
chlorinated polyethylene	H48	44.05	1.82×10^5 [a]	2.39×10^4	7.63
chlorinated polyethylene	CPE3	52.65	1.2×10^5 [a]	2.29×10^4	5.22
ethylene-vinyl acetate copolymer	EVA45	(45% vinyl acetate)	2.56×10^5 [a]	3.77×10^4	6.79
Cereclor 52	S52	53.1		437 [b]	
Cereclor 45	S45	45.7		395 [b]	
sec-octyl acetate (2-ethylhexyl acetate)	OC·AC		192		

[a] Relative to polystyrene, obtained by GPC. [b] Obtained by vapor-phase osmometry.

Table II

mixture	X_{12}, J·cm^{-3} 73.08 °C	83.5 °C	90 °C
OC·AC/S45	−4.2	−2.63	
OC·AC/S52	−6.5	−4.9	−3.2

All these titrations were performed at constant temperature.

The thermal expansion coefficients were determined by dilatometry as described by Orwoll and Flory.[14] The known amounts of polymer solids were placed in the dilatometer container, which has a total volume of about 1 cm^3. The container was then filled with clean Hg. Air bubbles were removed under vacuum, and the volume expansions of the materials were measured in the range 50–85 °C. The Hg and glass expansions were considered as explained by Orwoll and Flory.[14]

The thermal pressure coefficients of the polymers were estimated from their solubility parameters, which themselves are related to the cohesive energy density (CED) and hence to the strength of the internal pressure of the structural molecules. According to Allen et al.,[15] the internal pressure, P_i, at a given temperature is related to γ_i by

$$P_i \cong T\gamma_i \tag{16}$$

where

$$P_i = m(\mathrm{CED}) = m\delta_i^2 \tag{17}$$

or

$$m\delta_i^2 = T\gamma_i \tag{18}$$

where m for most polymers is close to 1. The solubility parameters can be obtained from the group contributions by using Small's theory.[16] Small calculated the molar attraction constant of different groups from vapor pressure and heats of vaporization data. His values were recently improved and updated by Hoy[17] and were used to calculate δ and, hence, γ of the polymeric materials at 25 °C. The values of γ calculated in this way for polymers for which data are available in the literature[18] agree within 10%.

The binary parameter S_2/S_1 was obtained by the method of group contributions.[19]

The X_{12} parameter was obtained by fitting eq 13 to the experimental heats of mixing of analogous materials as reported earlier.[2] The X_{12} thus obtained are given in Table II.

In the simulation of phase boundaries the temperature dependence of v_{sp}, α, and γ at atmospheric pressure must be considered.[10,14]

$$v_{sp} = v_{sp}{}^0 e^{\alpha\Delta T} \tag{19}$$

$$\alpha = \alpha_0 + \alpha_0{}^2(7 + 4\alpha_0 T)\Delta T/3 \tag{20}$$

$$\gamma = \gamma_0 - \gamma_0(1 + 2\alpha_0 T)\Delta T/T \tag{21}$$

The state parameters for pure components at 83.5 °C are given in Table III and were used in our calculations.

Simulation of the Spinodal

The spinodal condition is given by

$$\frac{\partial}{\partial\Phi_1}\left(\frac{\Delta\mu_1}{RT}\right)_{T,P} = \frac{\partial}{\partial\Phi_2}\left(\frac{\Delta\mu_2}{RT}\right)_{T,P} = 0 \tag{22}$$

The addition of Flory–Huggins combinatorial chemical potential of component one

$$\Delta\mu_1/RT = \ln\Phi_1 + (1 - r_1/r_2)\Phi_2 \tag{23}$$

to eq 15 and differentiating the assembly with respect to Φ_2 gives the spinodal temperature, T_{SP}, as

$$\frac{1}{T_{sp}}\left[P^*{}_1 D(1/\tilde{v}^2 + \tilde{P}_1) + X_{12}\left(\frac{2\Theta_2{}^2\Theta_1}{\tilde{v}\Phi_1\Phi_2}\right) - X_{12}D\frac{\Theta_2{}^2}{\tilde{v}^2}\right] = \left[(1/\Phi_1 - (1 - r_1/r_2))\frac{R}{V^*{}_1} + \frac{P^*{}_1}{T^*{}_1}\frac{D}{\tilde{v} - \tilde{v}^{2/3}}\frac{2\Theta_2{}^2\Theta_1}{\Phi_1\Phi_2}Q_{12}\right] \tag{24}$$

where

$$D = \partial\tilde{v}/\partial\Phi_2 = -\partial\tilde{v}/\partial\Phi_1 \tag{25}$$

$$\frac{\partial\tilde{v}}{\partial\Phi_2} = \left\{B - C\left(\frac{\tilde{P}}{\tilde{T}} + \frac{1}{\tilde{T}\tilde{v}^2}\right)\right\} \Big/ \left\{\frac{2}{\tilde{v}^3} - \frac{\tilde{T}}{3\tilde{v}^{5/3}}\frac{3\tilde{v}^{1/3} - 2}{(\tilde{v}^{1/3} - 1)^2}\right\} \tag{26}$$

$$B = \partial\tilde{P}/\partial\Phi_2 = P/P^{*2}[P^*{}_1 - P^*{}_2 - \Theta_2 X_{12}(1 - \Theta_1/\Phi_2)] \tag{27}$$

$$C = \partial\tilde{T}/\partial\Phi_2 = \tilde{T}B/\tilde{P} + (P^*{}_2\tilde{T}_2 - P^*{}_1\tilde{T}_1)/P^* \tag{28}$$

Table III
State Parameters for the Pure Materials at 83.5 °C

material	$10^4\alpha$, deg^{-1}	γ, J·cm^{-3}·deg^{-1}	v_{SP}, cm^3·g^{-1}	v^*_{SP}, cm^3·g^{-1}	$\tilde{v}$	T^*, K	P^*, J·cm^{-3} [a]
OC·AC	8.850	0.4893	1.2442	0.9877	1.2596	6067.21	276.930
S45	6.575	0.6708	0.9025	0.7506	1.2022	7200.98	345.854
S52	6.625	0.7360	0.8306	0.6901	1.2036	7167.45	380.305
EVA45	4.5103	0.8043	1.0636	0.9288	1.14509	9250.29	376.182
H48	4.4199	0.9544	0.81506	0.7134	1.1424	9384.51	444.342
CPE3	3.6546	0.9592	0.8089	0.7223	1.1198	10790.13	429.477

[a] 1 atm = 0.1013 J·cm^{-3} = 0.02422 cal·cm^{-3}.

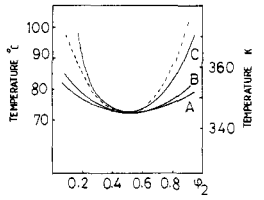

Figure 1. Simulated spinodal curves for EVA45–H48 mixtures using Flory's equation of state theory at the following conditions. (Temperature plotted against H48 fraction.) (A) $X_{12} = -4.2$ J·cm^{-3}, $Q_{12} = -0.0108$ J·cm^{-3}·deg^{-1}. (B) $X_{12} = -2.63$ J·cm^{-3}, $Q_{12} = -0.00678$ J·cm^{-3}·deg^{-1}. (C) $X_{12} = -0.5$ J·cm^{-3}, $Q_{12} = -0.00138$ J·cm^{-3}·deg^{-1}. ($S_2/S_1 = 0.98$, $r_2/r_1 = 1.68$, $V^*_1 = 200\,000$ cm^{-3}·mol^{-1}.) The dotted line is the experimental cloud point curve.

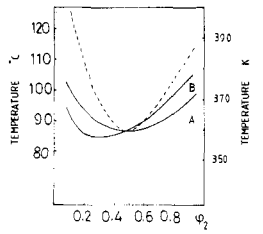

Figure 2. Simulated spinodal curves for EVA45–CPE3 mixtures at the following conditions. (Temperature plotted against fraction of CPE3.) (A) $X_{12} = -3.2$ J·cm^{-3}, $Q_{12} = -0.0063$ J·cm^{-3}·deg^{-1} (γ_2 was adjusted as described in the text to 0.8335 J·cm^{-3}·deg^{-1}). (B) $X_{12} = -3.2$ J·cm^{-3}, $Q_{12} = -0.0063$ J·cm^{-3}·deg^{-1} (γ_2 values were used as shown in Table III). ($S_2/S_1 = 1.03$, $r_1/r_2 = 2.86$.) The dotted line is the experimental cloud point curve.

These equations are more fully derived in the Appendix.

By use of eq 24–28 and data given in Tables II and III a number of spinodal curves at various conditions have been simulated. The effect of state parameters are generally in agreement with the findings of McMaster.[7]

The spinodal curves were simulated for EVA45–H48 mixtures by using the values of X_{12} shown in Table II for octyl acetate/S45 mixtures (S45 having a similar chlorine content to H48). A constant value of Q_{12} was chosen in each case to fit the theoretical spinodal to the experimental cloud point at the minimum of the cloud point curve. The full spinodal curve was then calculated. This was carried out with X_{12} values obtained from heats of mixing measurements at two temperatures in the region of the observed cloud point. The results are shown in Figure 1.

A larger negative X_{12} causes the spinodal curve to be flatter as the terms in X_{12} and Q_{12} dominate the spinodal equation. Both of the simulated curves are flatter than the experimental cloud point shown, an impossible situation as the spinodal should lie on or within the observed cloud point. A third spinodal was also simulated using an arbitrary, lower value of $X_{12} = -0.5$ and an appropriate value of Q_{12} obtained as above. This came closer to the observed cloud point. It should be pointed out that despite the known temperature dependence of ΔH and hence X_{12} within the range of temperatures covered by the calculation this treatment has used constant values for each simulation. We also consider that the heats of mixing and hence X_{12} values obtained at any given temperature could be critically dependent on the model system used to evaluate ΔH for a specific interaction showing a strong temperature dependence. We therefore conclude that the failure of the theory to include a temperature dependence of X_{12} and inadequacies in the model compounds used to evaluate ΔH values are the main reasons for the initial poor fit of the data.

The spinodal curve was also simulated for EVA45–CPE3 mixtures using the value of X_{12} shown in Table II for octyl acetate/S52 mixtures at 90 °C (S52 has a similar chlorine content to CPE3). The results are shown in Figure 2.

Again the curve is much flatter than the observed cloud point, which could be explained by the considerations mentioned earlier. The minimum in the cloud point curve also occurs at a different composition than in the spinodal. This can be corrected by choosing a different value of γ. The values of γ are only estimated to within 10%, and a variation in γ can affect the skew nature of the curve to a large extent even though it does not affect the temperature of the minimum in the curve very much. A curve using an adjusted value of γ is also shown in Figure 2.

The following summarizes the simulated spinodal shown in Figures 1 and 2 and the results of other simulation calculations not shown here: (1) Increasing the size of X_{12} (and the appropriate value of Q_{12}) causes the spinodal curve to be flatter. (2) Decreasing the molecular weight of either component, through its effect on V^* and/or r_1/r_2, increases the miscibility and skews the spinodal toward the appropriate component. (3) Varying the values of α alters both the position and the shape of the spinodal. Making the α values of the two materials more nearly equal tends to make the two polymers more miscible. (4) Varying the values of γ does not affect the temperature of the minimum of the spinodal very much but can affect the shape of the spinodal. This effect is also dependent on the values of α. (5) Altering the value of the ratio S_2/S_1 within a reasonable range has only a small effect on the shape of the spinodal, but large changes can significantly affect the results. (6) Our results show that the values of X_{12} obtained by fitting the heats of mixing of oligomeric and low molecular weight analogues are too large by a factor of 10. This is probably due to the temperature dependence of X_{12} and/or the inadequacy of the analogue model.

Similar calculations to the above could be pursued to find the binodal equation though this has not yet been done satisfactorily and appears to require further adjustable parameters. The cloud point curve should lie between the binodal and the spinodal, and the binodal would be a useful further comparison. In this case there is a further problem in simulating the binodal. As McMaster has shown,[7] the binodal is greatly affected by polydispersity whereas the spinodal is not. Our base polymers are very polydisperse.

Excess Volume Change on Mixing

The volume changes on mixing were calculated for EVA45–H48 and EVA45–CPE3 mixtures at the temperatures at which the heats of mixing of their model compounds were measured as given in ref 2. The values of X_{12} for the model compounds were assumed to be equivalent to those of analogous polymer mixtures at the same temperature. This assumption may not be completely correct. The volume change was calculated by[6]

$$\frac{\Delta V^M}{V^0} = \frac{\tilde{v} - \tilde{v}^0}{\tilde{v}^0} = \frac{\tilde{v}}{\tilde{v}^0} - 1 \tag{29}$$

where

$$\tilde{v}^0 = \Phi_1 \tilde{v}_1 + \Phi_2 \tilde{v}_2 \tag{30}$$

The values of $\tilde{v}$ used in these calculations were obtained using eq 5. The result is shown in Figure 3. It is evident that the volume changes on mixing of EVA45–CPE3 mixtures are larger in size than those of the EVA45–H48 mixtures, and also both values become smaller at higher temperatures. The theoretical value of $\Delta V^M/V^0$ for a 50/50% (w/w) blend of EVA45–CPE3 at 83.5 °C is −13.8

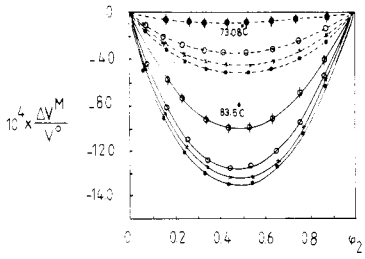

Figure 3. $\Delta V^M/V^0$ theoretically calculated, as described in the text, for EVA45–H48 (dotted lines) and EVA45–CPE3 (solid lines) mixtures at (●) 64.5 °C, (×) 73.08 °C and (○) 83.5 °C. Their values are plotted against the fraction of CPE3. The values corresponding to the curve marked by a slashed open circle are obtained from the EVA45–CPE3 data at 83.5 °C after correcting for the entropy dependence of the interaction term. The curve marked by a slashed darkened circle is obtained in the same way from data at 73.08 °C for the EVA45–H48 system.

$\times 10^{-4}$ in comparison with its experimental value of -7.2×10^{-4} obtained by measuring the $(dT/dP)_C$, the change in the cloud point produced by increased pressure, over the temperature range 82–96 °C (cf. ref 2). This discrepancy may be due to the assumption of Eichinger and Flory[6] that the volume changes on mixing should be less dependent upon entropy than the energy. This may not be true for the case where any specific interaction affects the entropy of mixing. Reducing the entropy contribution of the energy term by using the following equation

$$\bar{X}_{12} = X_{12} - TQ_{12}\tilde{v} \tag{31}$$

reduces the value of $\Delta V^M/V^0$ for the same blend at the same temperature to -10×10^{-4} and that at 90 °C to -9×10^{-4}. The remaining error may be due to an overestimation of X_{12}.

After making this entropy correction, we obtained a very small negative volume change on mixing for the EVA45–H48 mixture at 73.08 °C (just above the phase boundary, see Figure 3). This can only be explained by the fact that the reduced volume of the mixture, $\tilde{v}$, just above the phase boundary will not exceed the additivity volume of the mixture. Fourier transform infrared studies of the frequency shift in the carbonyl group have also indicated that the specific interaction will not be totally dissociated until temperatures well above the minimum in the cloud point curve.[3]

The important factor which affects the volume change on mixing is the reduced volume of the mixture, $\tilde{v}$, which can change the sign and magnitude of $\Delta V^M/V^0$. The value of $\tilde{v}$ in turn is related to X_{12} inasmuch as a strong specific interaction can outweigh the variational effect of S_2/S_1 and other related parameters. This is indirectly related to discrepancy between the theoretical and experimental volume change on mixing observed by Shih and Flory[21] for C_6H_6–PDMS mixtures. These authors without using eq 31 were unable to match the theoretical results to the experimental finding by any reasonable variation of the S_2/S_1 ratio.

Residual Free Energy Changes on Mixing

To calculate the residual free energy changes on mixing, G_M^R, eq 12–14 were used with

$$\bar{r}Nv^* = v^*_{sp} = W_1v^*_{1sp} + W_2v^*_{2sp} \tag{32}$$

The values of G_M^R at 73.08 and 83.5 °C for EVA45–H48 mixtures obtained in this way are given in Figure 4. Reductions in the free energy changes of the mixture at higher temperatures were observed. Introducing the entropy correction term $-v^*_{sp}TQ_{12}\Theta_1\Phi_2$ in eq 12, positive

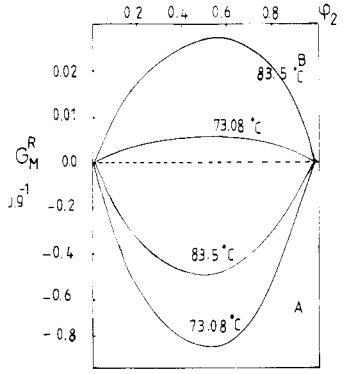

Figure 4. Theoretical residual free energy change on mixing of EVA45–H48 at 73.08 and 83.5 °C calculated from Flory's equation of state theory plotted against the fraction of H48. (A) X_{12} (73.08 °C) = −4.2 J·cm^{-3}, Q_{12} = 0.0 J·cm^{-3}·deg^{-1}; X_{12} (83.5 °C) = −2.62 J·cm^{-3}, Q_{12} = 0.0 J·cm^{-3}·deg^{-1}. (B) X_{12} (73.08 °C) = −4.2 J·cm^{-3}, Q_{12} = −0.0108 J·cm^{-3}·deg^{-1}; X_{12} (83.5 °C) = −2.62 J·cm^{-3}, Q_{12} = −0.00678 J·cm^{-3}·deg^{-1}.

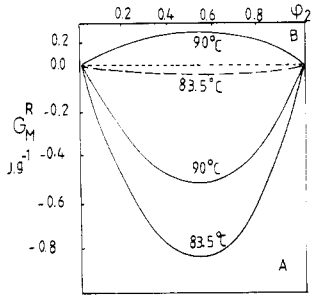

Figure 5. Theoretical residual free energy change of mixing of EVA45–CPE3 at 83.5 and 90 °C calculated from Flory's equation of state theory at the following conditions. (A) (—) X_{12} (83.5 °C) = −4.9 J·cm^{-3}, Q_{12} = 0.0 J·cm^{-3}·deg^{-1}; (– – –) X_{12} (83.5 °C) = −4.9 J·cm^{-3}, Q_{12} = −0.01 J·cm^{-3}·deg^{-1}; (—) X_{12} (90 °C) = −3.2 J·cm^{-3}, Q_{12} = 0.0 J·cm^{-3}·deg^{-1}. (B) (—) X_{12} (90 °C) = −3.2 J·cm^{-3}, Q_{12} = −0.0063 J·cm^{-3}·deg^{-1}.

values of G_M^R for the mixtures at 73.08 and 83.5 °C are obtained as shown in Figure 4. This trend conforms with the simulated spinodal and experimental cloud point curves. A similar calculation of G_M^R for EVA45–CPE3 at 83.5 °C correctly predicts a homogeneous mixture by using either Q_{12} = 0.0 or −0.01 J·cm^{-3}·deg^{-1} as shown in Figure 5. It also shows a homogeneous mixture at 90 °C when Q_{12} = 0.0 was used and inhomogeneous mixture at the same temperature when Q_{12} = −0.0063 J·cm^{-3}·g^{-1} was used.

Conclusion

When using the equation of state theory to simulate the spinodal curves of the polymer mixtures it is not possible to fit the calculations to the experimental results without using a noncombinatorial entropy correction term. This term using Q_{12} as an adjustable parameter can be used to fit the spinodal curve to the experimental results at the minimum of the cloud point curve.

If we obtain an interactional parameter, X_{12}, from the heats of mixing of low molecular weight analogues, and adjust the value of Q_{12} as described, then the full spinodal curves can be calculated. The resultant curve is however much flatter than the observed cloud point curve. One needs to use a much smaller value of X_{12} (and thus also Q_{12}) in order to fit the curves. This is attributed to the temperature dependence of X_{12} and/or differences between the analogues and the polymers themselves.

In a similar way the calculated volume changes on mixing are overestimated. If we take into account the Q_{12} term, volume changes closer to measured values can be obtained.

Appendix

The chemical potential of component 1 in the mixture is given by

$$\Delta\mu_1/RT = \ln \Phi_1 + (1 - r_1/r_2)\Phi_2 + P^*_1V^*_1/RT[3\tilde{T}_1 \ln (\tilde{v}_1^{1/3} - 1)/(\tilde{v}^{1/3} - 1) + 1/\tilde{v}_1 - 1/\tilde{v} + \tilde{P}_1(\tilde{v} - \tilde{v}_1)] + V^*_1X_{12}\Theta_2^2/RT\tilde{v} - V^*_1Q_{12}\Theta_2^2/R \quad (A.1)$$

Applying the spinodal condition, $\partial/\partial\Phi_2(\Delta\mu_1/RT) = 0$, to this equation yields

$$\partial/\partial\Phi_2(\Delta\mu_1/RT) = -1/\Phi_1 + (1 - r_1/r_2) + (P^*_1V^*_1/RT^*_1)(-D/(\tilde{v} - \tilde{v}^{2/3})) + P^*_1V^*_1D/RT\tilde{v}^2 + PV^*_1D/RT + V^*_1X_{12}2\Theta_2^2\Theta_1/RT\tilde{v}\Phi_1\Phi_2 - V^*_1X_{12}D\Theta_2^2/RT\tilde{v}^2 - V^*_1Q_{12}2\Theta_2^2\Theta_1/R\Phi_1\Phi_2 \quad (A.2)$$

where (see eq 11)

$$\partial\Theta_2/\partial\Phi_2 = \Theta_1\Theta_2/\Phi_1\Phi_2 \quad (A.3)$$

and

$$\partial\tilde{v}/\partial\Phi_2 = D \quad (A.4)$$

By differentiating eq 4 in respect of Φ_2, we obtain

$$\left\{\left(\frac{\partial\tilde{P}}{\partial\Phi_2}\tilde{v} + \tilde{P}\frac{\partial\tilde{v}}{\partial\Phi_2}\right)\tilde{T} - \tilde{P}\tilde{v}\frac{\partial\tilde{T}}{\partial\Phi_2}\right\} \Big/ \tilde{T}^2 = \left\{\tilde{v}^{-2/3}(\tilde{v}^{1/3} - 1)\frac{\partial\tilde{v}}{\partial\Phi_2} - \tilde{v}^{-1/3}\frac{\partial\tilde{v}}{\partial\Phi_2}\right\} \Big/ 3(\tilde{v}^{1/3} - 1)^2 + \left\{\frac{\partial\tilde{v}}{\partial\Phi_2}\tilde{T} + \tilde{v}\frac{\partial\tilde{T}}{\partial\Phi_2}\right\} \Big/ (\tilde{T}\tilde{v})^2 \quad (A.5)$$

Multiplying both sides by $\tilde{T}/\tilde{v}$ and rearranging we find

$$\frac{\partial\tilde{v}}{\partial\Phi_2} = \left\{\frac{\partial\tilde{P}}{\partial\Phi_2} - \frac{\partial\tilde{T}}{\partial\Phi_2}\left(\frac{\tilde{P}}{\tilde{T}} + \frac{1}{\tilde{T}\tilde{v}^2}\right)\right\} \Big/ \left\{\frac{2}{\tilde{v}^3} - \frac{\tilde{T}(3\tilde{v}^{1/3} - 2)}{3\tilde{v}^{5/3}(\tilde{v}^{1/3} - 1)^2}\right\} \quad (A.6)$$

To obtain $\partial\tilde{P}/\partial\Phi_2$ eq 9 is differentiated as follows:

$$\frac{-P\dfrac{\partial\tilde{P}}{\partial\Phi_2}}{\tilde{P}^2} = -P^*_1 + P^*_2 + \Theta_2X_{12} - \Theta_1\Theta_2X_{12}/\Phi_1\Phi_2 \quad (A.7)$$

or

$$\frac{\partial\tilde{P}}{\partial\Phi_2} = \frac{P}{P^{*2}}[P^*_1 - P^*_2 - \Theta_2X_{12}(1 - \Theta_1/\Phi_2)] \quad (A.8)$$

To obtain $\partial\tilde{T}/\partial\Phi_2$ eq 7 can be differentiated as follows:

$$\tilde{T} = \frac{T}{P}\tilde{P}\left(\frac{\Phi_1P^*_1}{T^*_1} + \frac{\Phi_2P^*_2}{T^*_2}\right)$$

$$\frac{\partial\tilde{T}}{\partial\Phi_2} = \frac{T}{P}\frac{\partial\tilde{P}}{\partial\Phi_2}\left(\frac{\Phi_1P^*_1}{T^*_1} + \frac{\Phi_2P^*_2}{T^*_2}\right) + \frac{T}{P}\tilde{P}\left(-\frac{P^*_1}{T^*_1} + \frac{P^*_2}{T^*_2}\right) \quad (A.9)$$

or

$$\frac{\partial\tilde{T}}{\partial\Phi_2} = \frac{\tilde{T}}{\tilde{P}}\frac{\partial\tilde{P}}{\partial\Phi_2} + \frac{T}{P^*}\left(\frac{P^*_2}{T^*_2} - \frac{P^*_1}{T^*_1}\right) \quad (A.10)$$

or simply

$$\frac{\partial\tilde{T}}{\partial\Phi_2} = \frac{\tilde{T}}{\tilde{P}}\frac{\partial\tilde{P}}{\partial\Phi_2} + \frac{P^*_2\tilde{T}_2 - P^*_1\tilde{T}_1}{P^*} \quad (A.11)$$

Substituting eq A.8 and A.11 into eq A.6 will give $\partial\tilde{v}/\partial\Phi_2$ (D in the spinodal equation).

Glossary

d	density
G^R_M	reduced free energy of mixing
ΔH_M	reduced enthalpy of mixing
P	pressure
$\tilde{P}_i$	reduced pressure of species i
P^*_i	hard core pressure of species i
$\tilde{P}$	reduced pressure of mixture
P^*	hard core pressure of mixture
Q_{12}	interaction entropy parameter
$\bar{r}N$	average number of segments in the mixture
R	gas constant
r_i	chain length of molecule i
S_i	number of contact sites per segment in species i
ΔS^R_M	reduced entropy of mixing
T	temperature
$\tilde{T}_i$	reduced temperature of species i
T^*_i	hard core temperature of species i
$\tilde{T}$	reduced temperature of mixture
T^*	hard core temperature of mixture
V^*_1	molar hard core volume of component 1
v_{sp}	specific volume of component i
$\tilde{v}_i$	reduced volume of component i
v^*_i	hard core volume of component i
$\tilde{v}$	reduced volume of mixture
v^*	hard core volume of mixture
W_i	weight fraction of species i
X_{12}	interactional parameter
$\bar{X}_{12}$	interactional energy parameter
α	thermal expansion coefficient
γ	thermal pressure coefficient
δ	solubility parameter
Φ_i	segment fraction of species i
Θ_i	site fraction of species i
$\Delta\mu_i$	chemical potential of component i

Registry No. (Ethylene)·(vinyl acetate) (copolymer), 24937-78-8.

References and Notes

(1) D. J. Walsh, J. S. Higgins, and S. Rostami, *Macromolecules*, **16**, 388 (1983).
(2) D. J. Walsh, J. S. Higgins, S. Rostami, and K. Weraperama, *Macromolecules*, **16**, 391 (1983).
(3) M. M. Coleman, E. J. Maskala, P. C. Painter, D. J. Walsh, and S. Rostami, *Polymer*, **24**, 1410 (1983).
(4) P. J. Flory, R. A. Orwoll, and A. Vriji, *J. Am. Chem. Soc.*, **86**, 3507 (1964).
(5) P. J. Flory, *J. Am. Chem. Soc.*, **87**, 1833 (1965).
(6) B. E. Eichinger and P. J. Flory, *Trans. Faraday Soc.*, **64**, 2035 (1968).
(7) L. P. McMaster, *Macromolecules*, **6**, 760 (1973).
(8) O. Olabisi, *Macromolecules*, **18**, 316 (1975).
(9) G. ten Brinke, A. Eshuis, E. Roerdenk, and G. Challa, *Macromolecules*, **14**, 867 (1981).
(10) Zhikuan Chai, Sun Rouna, D. J. Walsh, and J. S. Higgins, *Polymer*, **24**, 263 (1983).
(11) Zhikuan Chai and D. J. Walsh, *Makromol. Chem.*, **184**, 1459 (1983).
(12) S. Rostami, Ph.D. Thesis, Imperial College, London, 1983.
(13) ASTM D 1505-68, 1159 (1971).
(14) R. A. Orwoll and P. J. Flory, *J. Am. Chem. Soc.*, **89**, 6814 (1967).
(15) G. Allen, G. Gee, D. Mangaray, D. Sins, and G. J. Wilson, *Polymer*, **1**, 467 (1960).
(16) P. A. Small, *J. Appl. Chem.*, **3**, 71 (1953).
(17) K. L. Hoy, *J. Paint Technol.*, **42**, 76 (1970).
(18) J. Brandrup and E. H. Imergut, "Polymer Handbook", Wiley, New York, 1975.
(19) A. Bondi, *J. Phys. Chem.*, **68**, 441 (1964).
(20) A. Abe and P. J. Flory, *J. Am. Chem. Soc.*, **87**, 1838 (1965).
(21) H. Shih and P. J. Flory, *Macromolecules*, **5**, 758 (1972).